J|A|C|S COMMUNICATIONS

Published on Web 09/10/2009

Controlled Formation of Concave Tetrahedral/Trigonal Bipyramidal Palladium Nanocrystals

Xiaoqing Huang, Shaoheng Tang, Huihui Zhang, Zhiyou Zhou, and Nanfeng Zheng*

State Key Laboratory for Physical Chemistry of Solid Surfaces and Department of Chemistry, College of Chemistry and Chemical Engineering, Xiamen University, Xiamen 361005, China

Received July 16, 2009; E-mail: nfzheng@xmu.edu.cn

In the past decade, the controlled synthesis of noble metallic nanocrystals with uniform geometries has attracted enormous interest, because it could provide an effective route for tuning the catalytic, optical, electronic, or magnetic properties of metals.[1−3] Noble metal nanocrystals with a large variety of shapes have been synthesized by different techniques, such as template-directed fabrication,[4,5] electrochemical,[6,7] or chemical synthesis.[8−12] However, the majority of metal nanocrystals that have been prepared to date are spheres, cubes,[13,14] tetrahedra,[15] octahedra,[16] and rods/wires,[17−19] limited to the flat or convex shapes. Reports on the synthesis of concave metal nanocrystals are rare.[20]

We report here a facile synthetic strategy to prepare concave polyhedral Pd nanocrystals. The as-prepared Pd nanocrystals are enclosed by {111} and reactive {110} facets. The electrocatalytic activity of the concave nanocrystals in formic acid oxidation exhibits dependency on the percentage of {110} facets which are controllable by varying reaction conditions.

In a typical synthesis of concave Pd nanocrystals, $Pd(acac)_2$, PVP, and formaldehyde solution were mixed together with benzyl alcohol. The resulting homogeneous solution was transferred to a Teflon-lined stainless-steel autoclave. The sealed vessel was then heated at 100 °C for 8 h. The resulting products were collected by centrifugation and washed several times with ethanol and acetone.

The representative electron microscopic images of the as-made Pd nanocrystals are illustrated in Figure 1. It was clearly revealed that concave polyhedral nanocrystals were the dominant products with a typical yield of >80%. The concave nanocrystals had a uniform side length and were present in two forms with tetrahedral and trigonal bipyramidal shapes which were in a ratio of ∼3:1 (Figure S1). Their side lengths were 45 ± 2 nm and 35 ± 2 nm, respectively. The concave feature of the as-prepared nanocrystals was also confirmed by the HAADF-STEM and SEM analysis (Figure 1c, 1d). The most striking feature of the as-made concave nanocrystals is that the concave surfaces are essentially {110} whose surface energies are however the highest among all low-index facets (i.e., {111}, {100}, and {110}) of fcc metals.[21]

Both the selected area electron diffraction (SAED) and high resolution TEM (HRTEM) (Figure 1e, f) measurements on single concave tetrahedra clearly indicated their single-crystalline nature. While the SAED pattern (Figure 1e inset) was indexed to the [111] zone axis of an fcc Pd single crystal, the HRTEM images showed lattice fringes with an interplanar spacing of 0.139 nm, corresponding to {220} planes of fcc Pd. These fringes were running along the edge of the tetrahedron. Together with the SAED and HRTEM, the HAADF-STEM and SEM analysis suggested good geometric agreement between the concave tetrahedral nanocrystals and the model shown in Figure 1e. The model can be better visualized as an excavated tetrahedron with a trigonal pyramid excavated at the center of each face of the tetrahedron. Each cut-out pyramid has a {111} face and three {110} faces exposed. As a result, each excavated tetrahedral nanocrystal consists of four {111} faces shaped in a hollow equilateral triangle and 12 isosceles triangle-like {110} faces concave toward the center of the tetrahedron. The outer and inner side lengths of the hollow equilateral triangle face determine the degree of concavity of the nanocrystals and therefore the fraction of {110} facets in the as-prepared concave tetrahedra (Figure S2, Table S1). While the concave tetrahedra are single-crystalline, the concave trigonal bipyramids are single twinned with a stacking fault along the {111} plane (Figure S3).[22,23] The presence of both {111} and {110} facets in the as-prepared concave nanocrystals was confirmed by the CO stripping experiments in both H_2SO_4 and $HClO_4$ solutions. The peaks observed in both CO stripping curves (Figure S4) are well attributed to the CO stripping on Pd (110) and (111) facets.[24]

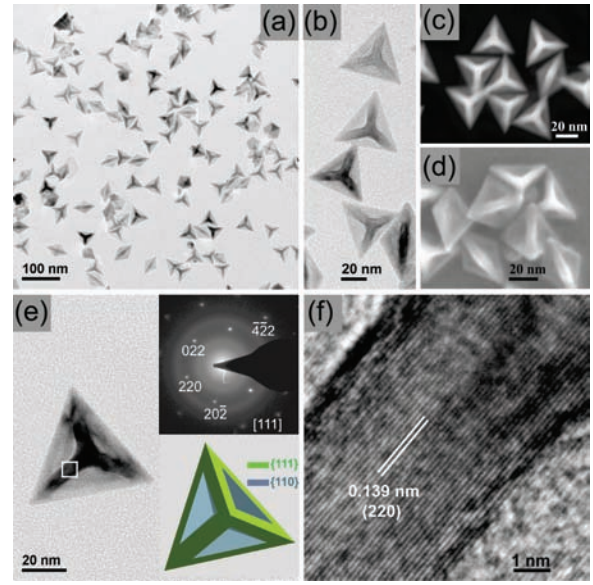

Figure 1. (a) Large-area and (b) enlarged TEM, (c) HAADF-STEM, and (d) SEM images of as-synthesized concave Pd nanocrystals. (e) High-magnification TEM image of a single concave tetrahedron. Top-right and bottom-right insets show the corresponding SAED pattern and the ideal structure model of the concave tetrahedron. (f) High-resolution TEM image of the squared area indicated in (e).

To better understand the formation process of concave polyhedra, the intermediate nanocrystals produced at different reaction times were investigated by TEM. Figure 2 details the morphological evolution of the Pd nanocrystals with the reaction time. The Pd polyhedra produced in a 1-h reaction had a side length of ∼16 nm (Figure S5). These nanocrystals continued to grow within 8 h. Their average side length was increased to 24 nm at 2 h, 38 nm at 4 h, and 45 nm at 8 h. Associated with the size enlargement, the concave feature was shaping up. While hardly observed at 1 h, the feature

10.1021/ja9059409 CCC: $40.75

became discernible at 2 h and evident at 4 h and thereafter. Beyond 8 h, no further change on both the size and morphology of the nanocrystals was observed. These results imply that the concave faces were developed at the very beginning and concomitant with the growth process. When formaldehyde was substituted with benzaldehyde, the reactions also led to the formation of concave Pd nanocrystals, indicating the correlation of the concave structure formation to the aldehyde group (Figure S6).

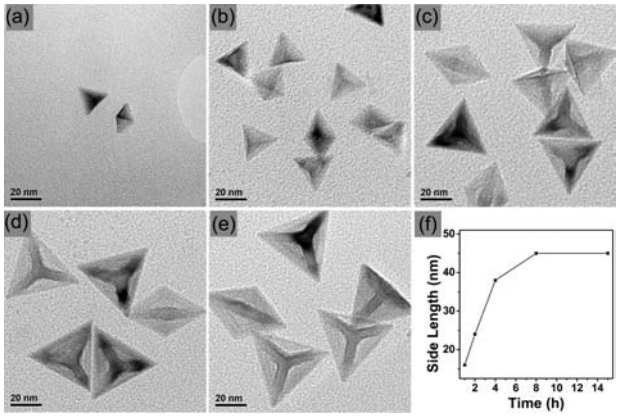

Figure 2. TEM images of the concave polyhedral Pd nanocrystals produced in (a) 1.0-, (b) 2.0-, (c) 4.0-, (d) 8.0-, and (e) 15-h reactions. (f) Summary curve of the time-dependent side length.

While the absence of formaldehyde led to the formation of Pd nanocrystals with mixed morphologies (Figure S7), the concentration of formaldehyde controlled the degree of concavity of the nanocrystals. When the formaldehyde solution (40%) supplied was reduced from 0.1 to 0.07, 0.04, 0.02, and 0.01 mL, the concave feature gradually faded out and finally disappeared (Figures S8, S9). Based on the ideal concave tetrahedral model, the percentage of {110} facets was approximately calculated decreasing from 44% to 0 (Table S1). In contrast, the concave degree was almost unaffected by increasing the amount of formaldehyde solution from 0.1 to 0.5 mL.

In addition to the formaldehyde concentration, the degree of concavity of the as-prepared nanocrystals depended on the reaction temperatures. The reactions under the same conditions but at higher temperatures yielded particles with a smaller concave fraction (Figure S10). The average size of the concave polyhdedra was experimentally tunable by varying the concentration of precursor and the solvent (Figure S11). Reducing the $Pd(acac)_2$ concentration from 16 to 8 mM led to the decreasing average size from 45 to 34 nm. Increasing the $Pd(acac)_2$ concentration to 33 mM produced nanocrystals with an average size of 58 nm. When DMF was used as the solvent, the size of the tetrahedral nanocrystals was further increased to 78 nm.

The existence of reactive {110} facets in the as-prepared concave nanocrystals has motivated us to investigate their catalytic properties. Electrocatalytic oxidation of formic acid was chosen for comparison studies on three types of nanocrystals with comparable size but different percentages of {110}. The nanocrystals were synthesized under the same conditions but using different amounts of formaldehyde (Table S1). Based on TEM measurements, the percentages of {110} surfaces were calculated as 0, 10, and 44%, increasing with the degree of concavity (Figure 3a−c). The maximum current densities of these nanocrystals were measured as 127, 193, and 273 mA/mg, respectively (Figure 3d). These results clearly demonstrate that the catalytic activity enhanced with the increase in the percentage of {110} facets in the concave nanocrystals.

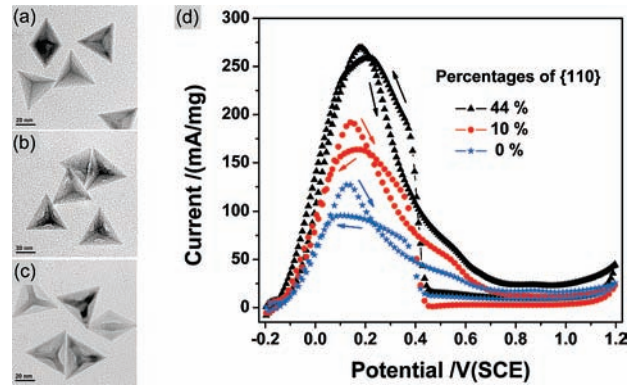

Figure 3. (a−c) TEM images and (d) electrocatalytic properties of Pd nanocrystals with different percentages of {110} facets. The CV curves were recorded in 0.5 M H_2SO_4 + 0.25 M HCOOH solution at a scan rate of 50 mV/s.

In conclusion, concave Pd nanocrystals with uniform diameter were successfully prepared in the presence of formaldehyde. The as-made concave Pd nanocrystals are bound with {111} and {110}. Their electrocatalytic activity increases with the percentage of {110} facets which correlates with their degree of concavity.

Acknowledgment. We thank NSFC (20871100, 20721001), NSFC for Distinguished Young Investigator Grant, MSTC (92009CB930703), RFDP(200803841010), NSF of Fujian for Distinguished Young Investigator Grant (2009J06005), and the Key Scientific Project of Fujian Province (2009HZ0002-1).

Supporting Information Available: Experimental details and data. This material is available free of charge via the Internet at http://pubs.acs.org.

References

(1) Burda, C.; Chen, X. B.; Narayanan, R.; El-Sayed, M. A. *Chem. Rev.* **2005**, *105*, 1025.
(2) Tao, A. R.; Habas, S.; Yang, P. D. *Small* **2008**, *4*, 310.
(3) Xia, Y. N.; Xiong, Y. J.; Lim, B.; Skrabalak, S. E. *Angew. Chem., Int. Ed.* **2009**, *48*, 60.
(4) Mayers, B.; Jiang, X. C.; Sunderland, D.; Cattle, B.; Xia, Y. N. *J. Am. Chem. Soc.* **2003**, *125*, 13364.
(5) Lee, K. B.; Lee, S. M.; Cheon, J. *Adv. Mater.* **2001**, *13*, 517.
(6) Liang, C. H.; Terabe, K.; Tsuruoka, T.; Osada, M.; Hasegawa, T.; Aono, M. *Adv. Funct. Mater.* **2007**, *17*, 1466.
(7) Tian, N.; Zhou, Z. Y.; Sun, S. G.; Ding, Y.; Wang, Z. L. *Science* **2007**, *316*, 732.
(8) Peng, Z. M.; Yang, H. *J. Am. Chem. Soc.* **2009**, *131*, 7542.
(9) Sanchez-Iglesias, A.; Pastoriza-Santos, I.; Perez-Juste, J.; Rodriguez-Gonzalez, B.; Garcia de Abajo, F. J.; Liz-Marzan, L. M. *Adv. Mater.* **2006**, *18*, 2529.
(10) Wang, C.; Daimon, H.; Onodera, T.; Koda, T.; Sun, S. H. *Angew. Chem., Int. Ed.* **2008**, *47*, 3588.
(11) Ma, Y. Y.; Kuang, Q.; Jiang, Z. Y.; Xie, Z. X.; Huang, R. B.; Zheng, L. S. *Angew. Chem., Int. Ed.* **2008**, *47*, 8901.
(12) Kim, F.; Sohn, K.; Wu, J. S.; Huang, J. X. *J. Am. Chem. Soc.* **2008**, *130*, 14442.
(13) Huang, X. Q.; Zhang, H. H.; Guo, C. Y.; Zhou, Z. Y.; Zheng, N. F. *Angew. Chem., Int. Ed.* **2009**, *48*, 4808.
(14) Sun, Y. G.; Xia, Y. N. *Science* **2002**, *298*, 2176.
(15) Kim, F.; Connor, S.; Song, H.; Kuykendall, T.; Yang, P. D. *Angew. Chem., Int. Ed.* **2004**, *43*, 3673.
(16) Seo, D.; Park, J. C.; Song, H. *J. Am. Chem. Soc.* **2006**, *128*, 14863.
(17) Xia, Y. N.; Yang, P. D.; Sun, Y. G.; Wu, Y. Y.; Mayers, B.; Gates, B.; Yin, Y. D.; Kim, F.; Yan, Y. Q. *Adv. Mater.* **2003**, *15*, 353.
(18) Sau, T. K.; Murphy, C. J. *J. Am. Chem. Soc.* **2004**, *126*, 8648.
(19) Huang, X. Q.; Zheng, N. F. *J. Am. Chem. Soc.* **2009**, *131*, 4602.
(20) Zhou, Z. Y.; Tian, N.; Huang, Z. Z.; Chen, D. J.; Sun, S. G. *Faraday Discuss.* **2008**, *140*, 81.
(21) Wang, Z. L. *J. Phys. Chem. B* **2000**, *104*, 1153.
(22) Liu, M. Z.; Guyot-Sionnest, P. *J. Phys. Chem. B* **2005**, *109*, 22192.
(23) Wiley, B. J.; Xiong, Y. J.; Li, Z. Y.; Yin, Y. D.; Xia, Y. N. *Nano Lett.* **2006**, *6*, 765.
(24) Hara, M.; Linke, U.; Wandlowski, T. *Electrochim. Acta* **2007**, *52*, 5733.

JA9059409